JOURNAL OF VIROLOGY, Mar. 1997, p. 1747–1756 Vol. 71, No. 3
0022-538X/97/$04.00+0

The Cellular Transcription Factor SP1 and an Unknown Cellular Protein Are Required To Mediate Rep Protein Activation of the Adeno-Associated Virus p19 Promoter

DANIEL J. PEREIRA[1, 2] AND NICHOLAS MUZYCZKA[2]*

Department of Genetics and Molecular Microbiology, State University of New York at Stony Brook, Stony Brook, New York 11794,[1] and Department of Molecular Genetics and Microbiology, Gene Therapy Center, University of Florida, Gainesville, Florida 32610[2]

Received 18 September 1996/Accepted 16 November 1996

Control of adeno-associated virus (AAV) transcription from the three AAV promoters (p5, p19, and p40) requires the adenovirus E1a protein and the AAV nonstructural (Rep) proteins. The Rep proteins have been shown to repress the AAV p5 promoter yet facilitate activation of the p19 and p40 promoters during a productive infection. To elucidate the mechanism of promoter regulation by the AAV Rep proteins, the cellular factors involved in mediating Rep activation of the p19 promoter were characterized. A series of protein-DNA binding experiments using extracts derived from uninfected HeLa cells was performed to identify cellular factors that bind to the p19 promoter. Electrophoretic mobility shift assays, DNase I protection analyses, and UV cross-linking experiments demonstrated specific interactions with the cellular factor SP1 (or an SP1-like protein) at positions −50 and −130 relative to the start of p19 transcription. Additionally, an unknown cellular protein (cellular AAV activating protein [cAAP]) with an approximate molecular mass of 34 kDa was found to interact with a CArG-like element at position −140. Mutational analysis of the p19 promoter suggested that the SP1 site at −50 and the cAAP site at −140 were necessary to mediate Rep activation of p19. Antibody precipitation experiments demonstrated that Rep-SP1 protein complexes can exist in vivo. Although Rep was demonstrated to interact with p19 DNA directly, the affinity of Rep binding was much lower than that seen for the Rep binding elements within the terminal repeat and the p5 promoter. Furthermore, the interaction of purified Rep68 with the p19 promoter in vitro was negligible unless purified SP1 was also added to the reaction. Thus, the ability of Rep to transactivate the p19 promoter is likely to involve SP1-Rep protein contacts that facilitate Rep interaction with p19 DNA.

Adeno-associated virus (AAV) is classified as a nonautonomous parvovirus, and under most conditions AAV requires the presence of a helper virus, i.e., adenovirus (Ad), for a productive infection (8, 40). The 4.7-kb genome of AAV contains two open reading frames, *rep* and *cap*. AAV uses three promoters to regulate the expression of these open reading frames (16, 17). The promoters at map positions 5 and 19 (p5 and p19) regulate the expression of the nonstructural (Rep) proteins and encode four overlapping proteins with approximate molecular masses of 78, 68, 52, and 40 kDa (41, 52, 55). The structural (Cap) proteins are derived from transcripts initiated at the p40 promoter (3, 4, 26).

In the absence of helper virus, AAV transcription is not typically observed (12, 32, 33). The presence of Ad helper results in activation of AAV promoter activity (9, 33, 54). The Ad early region 1a protein (E1a) functions to activate the p5 and p19 promoters and is facilitated by interactions with the p5-bound cellular proteins YY1 and major late transcription factor (9, 34, 50). The components required for E1a activation at p19 are not known. The additional Ad genes required as Ad helper functions facilitate AAV gene expression posttranscriptionally by cytoplasmic transport and stabilization of AAV messages (46, 47, 57).

Genetic analysis of the AAV genome has demonstrated that the p5 Rep proteins (Rep78 and Rep68) are required to regulate transcription from all three promoters and to replicate the viral DNA (20, 53). Several biochemical properties have been characterized for the p5 Rep proteins during replication; these include site-specific endonuclease (24, 51), DNA helicase (24, 58), and DNA binding (24, 25, 38) activities. In the absence of Ad, Rep has been shown to repress both p5 and p19 transcription (21, 30). Repression of p5 is mediated in part by direct binding of Rep78 or Rep68 to the p5 Rep binding element (RBE) (31, 43). In the presence of helper virus, Rep78/68 transactivation of the p19 and p40 promoters is dependent on the presence of the RBEs in the p5 promoter and the terminal repeat (TR) (36, 43).

The functions of the p19 Rep proteins, Rep52 and Rep40, in transcriptional regulation are not clearly defined. It has been reported that these proteins function as repressors of p5 activity in the absence of helper virus (21, 30). In the presence of helper virus, however, Rep52 and Rep40 act to attenuate p5 activity by antagonizing Rep78 and Rep68 repression (43). Mutational analysis of the *rep* coding region has yielded several domains responsible for DNA binding, transactivation of the p19 and p40 promoters, and repression of p5 (37, 59). DNA binding domains at both the N and C termini are necessary for transactivation and repression activities. Mutations in the nucleoside triphosphate binding domain have no effect on the repression and DNA binding activities but are required for transactivation. Finally, the p19 Rep proteins, Rep52 and Rep40, are missing N-terminal amino acid sequences required for binding the RBE. Thus, the p19 Rep proteins are likely to exert their effects through protein contacts with other cellular or viral proteins which have not yet been identified.

* Corresponding author. Mailing address: Department of Molecular Genetics and Microbiology, Gene Therapy Center, Box 100266 JHMHSC, University of Florida, Gainesville, FL 32610. Phone: (352) 392-8541. Fax: (352) 392-5914. E-mail: muzyczka@medmicro.med.ufl.edu.

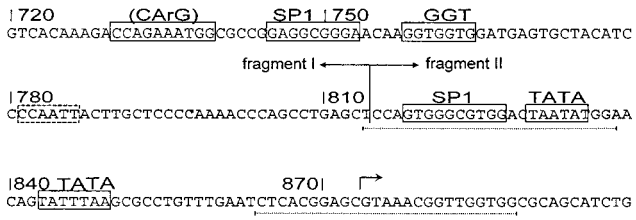

FIG. 1. Sequence of the p19 promoter. AAV nucleotides are indicated by vertical lines. The p19 initiation site is indicated by a bent arrow. Open boxes outline sequences with homology to SP1, CArG-like, GGT, and TATA transcription factor binding elements. Deletions of nt 720 to 749, 750 to 779, 810 to 839, and 840 to 869 have been shown previously to reduce p19 activity (36). In contrast, deletion of nt 780 to 809, including the CATT element (27) (dotted box), is not required for p19 promoter activity. Sequences with homology to the linear TR RBE are underlined by a dotted line (38). The boundary between fragments I and II, which were used in protein binding experiments, is indicated by arrows.

Although the viral and cellular interactions that regulate p5 activity have been characterized, nothing is known about similar interactions at the p19 promoter. In earlier studies, we used deletion analysis to demonstrate that four 30-bp regions in the p19 promoter were necessary for mediating Rep activation of p19 (Fig. 1, nucleotides [nt] 720 to 779 and nt 810 to 869). The aim of this study was to identify the proteins that were interacting with these regions and determine their contribution to p19 promoter activity. Our experiments demonstrated that two SP1 elements, one at position −50 relative to p19 transcript initiation and another at position −130, were both required for p19 promoter activity. Additionally, we have identified a novel protein with a molecular mass of approximately 34 kDa, which we have called the cellular AAV activating protein (cAAP), that interacts with a CArG-like element at position −140. Finally, evidence is provided that SP1 facilitates Rep induction of the p19 promoter by stabilizing Rep interactions with p19 DNA through direct protein-protein contacts made between SP1 and Rep78/68.

MATERIALS AND METHODS

Cell lines and transfections. Human A549 cells (ATCC CCL 185) were maintained in Dulbecco's modified essential medium (DMEM; Gibco BRL) containing 10% bovine calf serum (BCS) at 37°C in 100-mm-diameter culture dishes. HeLa suspension cells were grown in Joklik modified essential medium containing 10% BCS. Plasmid delivery was performed by using cationic liposomes made with DC-cholesterol and dioleoyl-L-α-phosphatidylethanolamine (DOPE; Avanti) as described previously (15). Liposomes (12 μg) were mixed with plasmid DNA in 2 ml of serum-free medium and put on the cells. Following a 3-h incubation at 37°C, 4 ml of DMEM containing 10% BCS and Ad type 2 at a multiplicity of infection of 5 was added. Sixteen hours postinfection, the medium was replaced with fresh DMEM containing 2% BCS, and cells were harvested 40 to 46 h postinfection.

Plasmids. Plasmid pIM45 contained AAV nt 145 to 4486 in a pBS M13+ vector (36). Mutants in the p19 promoter region were constructed in the background of pIM45 by using oligonucleotide-directed mutagenesis (29). The SP1-50, SP1-130, GGT-110, and CArG-140 elements were substituted with an *Xho*I restriction site and an amber termination codon (Table 1; Fig. 1). The SP1-130 and GGT-110 double mutant contained *Xho*I and *Xba*I restriction sites at the two positions, respectively, and an in-frame opal termination codon (Table 1; Fig. 1). A *Sac*II restriction site was introduced in place of each of the two p19 TATA elements (Table 1; Fig. 1).

The Rep helper plasmid, p19/40S, contains a series of nucleotide mutations downstream from the p19 and p40 initiation sites. These mutations, however, do not alter the amino acid composition of Rep but prevent the antisense riboprobe from completely annealing to these transcripts; this allows one to distinguish p19 transcription from p19/40S which is rep^+ and the p19 mutants in the pIM45 background (36). Plasmid pCMVRep78/68 encodes the AAV Rep78 and Rep68 proteins under the control of the human cytomegalovirus immediate-early promoter and has been described elsewhere (43).

Plasmid RP19 was used as the template for synthesis of p19 antisense transcripts used in the RNase protection assay. RP19 was constructed by inserting a *Sac*II/*Bam*HI fragment (AAV nt 814 to 1045) into homologous sites of pBS M13+ (Stratagene). The orientation of the AAV insert allowed the use of the T3 RNA polymerase promoter to synthesize p19 antisense transcripts. The probe when hybridized to p19 transcripts yields a 175-bp RNase-resistant fragment. The probe also hybridizes to transcripts from the p19/40S template; however, due to mismatches between AAV nt 941 and 959, RNase digestion yields 86- and 69-bp protected fragments. PLK215 (obtained from N. Reich, State University of New York at Stony Brook) was used to generate antisense RNA that detects the γ-actin transcripts. A *Bam*HI/*Hin*dIII fragment from mouse γ-actin cDNA was positioned in pSP64 to utilize the SP6 RNA polymerase promoter. The probe when hybridized to human γ-actin transcripts yields a 135-bp protected fragment.

Protein-DNA binding experiments. Probes were generated by PCR to amplify sequences within the p19 promoter from pIM45 and p19 promoter mutants. The PCR mixtures contained, in a volume of 75 μl, 50 mM KCl, 10 mM Tris-HCl (pH 8.8), 3 mM $MgCl_2$, 0.1% Triton X-100, 1.5 mM each dATP, dCTP, dGTP, and dTTP, 0.014 pM plasmid DNA, 100 pM ^{32}P 5′-end-labeled oligonucleotide, 100 pM unlabeled oligonucleotide, and 5 U of *Taq* DNA polymerase (Promega Biotech). The reactions were subjected to 27 cycles of 45 s at 94°C, 45 s at 59°C, and 30 s at 72°C. The probes then were purified on a 5% nondenaturing polyacrylamide gel. The primers used for amplification were 20 bases long and had their 5′ ends positioned at nt 687 and 906. A third 20-base primer with its 5′ end at nt 598 was used in place of the primer at nt 687 to synthesize the probe for DNase footprinting experiments. All primers were 5′ labeled with polynucleotide kinase (New England Biolabs) and [γ-^{32}P]ATP (3,000 Ci/mmol). Probes used in the electrophoretic mobility shift assays (EMSAs) were digested with *Sac*I to generate two fragments of 127 bp (fragment I, AAV nt 687 to 814) and 92 bp (fragment II, AAV nt 814 to 906). These fragments were separated by polyacrylamide gel electrophoresis (PAGE) and used in separate binding reactions.

Crude nuclear extracts were prepared from 3 liters of HeLa suspension cultures as described previously (13). Pure human SP1 was obtained from Promega and supplied at 1 footprinting unit per μl. Rep68 was prepared from a baculovirus overexpression system and purified through DNA affinity chromatography as described previously (36).

EMSAs were performed in 20-μl reactions containing 20 mM HEPES (pH 7.9), 5 mM $MgCl_2$, 50 mM NaCl, 10 μM $ZnSO_4$ and 3 μg of sonicated salmon sperm DNA. The 5′-end-labeled DNA was incubated with various amounts of a crude nuclear extract. The reaction mixtures were incubated for 20 min at room temperature and were then loaded onto a 4 or 5% polyacrylamide gel and electrophoresed at room temperature in 0.5× TBE (45 mM Tris-HCl, 89 mM boric acid, 1 mM EDTA) for 2 to 3 h at 9 V/cm. In some experiments, 5 mM $MgCl_2$ was included in the gel running buffer. The oligonucleotide competitor containing SP1 sites consisted of three tandem binding SP1 sites (6) and had the sequence 5′-GGGCGGGGCGCGGCGGGGCGGGGCGGGGC. An oligonucleotide containing the c-*fos* serum response element (SRE) was also used as a competitor in some reactions and had the sequence 5′-GGATGTCCATATTA GGACATCT (56). Antibodies specific for human SP1 (Santa Cruz Biotechnology) and all four AAV Rep proteins (anti-52/40) (22) were used in antibody addition EMSAs.

The reaction conditions for DNase I footprinting experiments were identical to those for the EMSAs except that the reaction volume was increased to 50 μl and 1 μg of poly(dI-dC) was used as the nonspecific competitor. Following

TABLE 1. Oligonucleotides used for mutagenesis[a]

AAV nt	Sequence	Substitution
717–752	cgcgtcacaaagaCTCGAGCC**TAG**gccggaggccgg	CArG-140
732–767	agaaatggcgccgCTCGAGCT**TAG**aaggtggtggat	SP1-130
743–777	gaggcgggaacaaCTCGAGG**TAG**gagtgctacat	GGT-110
806–841	gcctgagctccagCTCGAG**TAG**actaatatggaac	SP1-50
819–853	tgggcgtggacCCGCGGggaacagta	TATA-35
843–869	tatggaacagCCGCGGtgcgcctgttt	TATA-30
733–780	gaaatggcgccgTCTCGAG**TGA**caaTTCTAGATCCagtgctacatcc	SP1-130/GGT-110

[a] Nucleotide changes are indicated in uppercase. In-frame amber codons (opal for the SP1-130/GGT-110 mutant) are in boldface.

incubation at room temperature for 20 min, 50 μl of a solution containing 10 mM $MgCl_2$ and 5 mM $CaCl_2$ was added to the reaction mixture, which was then put on ice for 5 min. To these reaction mixtures, 0.2 U of DNase I (Worthington Biochemicals) was added, and incubation was continued on ice for 2 min. The reaction was stopped by the addition of 90 μl of 20 mM EDTA, 1% sodium dodecyl sulfate (SDS), 0.2 M NaCl, and 1.1 mg of carrier tRNA per ml. The reactions were extracted with phenol-chloroform (1:1) and precipitated with ethanol. The reaction products were analyzed on a sequencing gel alongside a Maxam and Gilbert G+A sequencing ladder of the same probe (2).

The probes used for UV cross-linking experiments were uniformly labeled with 300 μCi of [α-^{32}P]dCTP (3,000 Ci/mmol). Reaction conditions were identical to those used in the EMSAs. Following incubation for 15 min at 25°C, the reaction mixtures were exposed to UV light (λ = 254 nm) for 30 min. This was followed by the addition of $CaCl_2$ to a final concentration of 25 mM, 2 U of DNase I, and 1 U of micrococcal nuclease and incubation at 37°C for 30 min. An equal volume of 2× SDS-PAGE loading buffer was added, and the reaction products were boiled for 5 min. The samples then were subjected to SDS-PAGE (10% polyacrylamide gel) along with ^{14}C-labeled protein markers (Amersham).

To determine the ratio of dissociation constants (K_ds) of the TR, p5, p19, and p40 substrates, a high-substrate-concentration competition binding analysis was performed essentially as described previously (39). Promoter fragments used as competitors were synthesized by PCR using pIM45 as the template for amplification, and the p19 primers used were those (described above) that had their 5′ ends at nt 687 or 906. The p5 and p40 primer pairs were 20 bp long and had their 5′ ends at nt 136 and 305 and at nt 1666 and 1850, respectively. Primers used to amplify promoter sequences for use as competitors were not end labeled, and the reaction was scaled up 10-fold. Following amplification, the promoter fragments were gel purified by electrophoresis on a 1% agarose gel. The molar concentration of each competitor was determined by A_{260}. The terminal repeat RBE oligonucleotide substrate has been described previously (39). It had the sequence 5′-ctagattaCTCAGTGAGCGAGCGAGCGCGCAGAGAGGGctgtc, where the uppercase letters represent AAV TR sequences and the lowercase letters are random sequences used to extend the length of the substrate. A corresponding minus strand was annealed to this oligonucleotide by mixing equimolar amounts of each in a volume of 50 μl containing 0.1 M NaCl and 1 mM EDTA, heating at 65°C for 5 min and cooling to room temperature. The oligonucleotides were 5′-end labeled with [γ-^{32}P]ATP and precipitated with ethanol. Then 0.025 pmol of labeled RBE substrate was incubated with 60 ng of Rep68 in a reaction volume of 20 μl containing 20 mM HEPES (pH 7.9), 100 mM NaCl, 20% glycerol, 5 mM $MgCl_2$, 0.2 mM EDTA, 0.5 mM dithiothreitol, and 1 μg of poly(dI-dC). The reaction mixtures were incubated for 20 min at room temperature and analyzed on a 5% polyacrylamide gel containing 0.5× TBE. Bands corresponding to bound and free DNA were cut from the gel, and radioactivity was measured in a scintillation counter. The fraction of bound substrate was then plotted as a function of picomoles of unlabeled competitor. The ratio of the K_ds was determined by calculating the ratio of homologous competitor (TR competitor) to heterologous competitor (p5 substrate) that was required to reduce the fraction of labeled TR substrate that was bound by 10% of the starting value. The ratios for the p19 and p40 competitors could not be measured in this way due to the low affinity of these substrates for Rep68. The ratio of these K_ds therefore was determined by comparison to the p5 competitor and extrapolation to the TR RBE.

RNA isolation. Forty hours postinfection, the cells were scraped into the medium and washed with phosphate-buffered saline. One-tenth of the cells were used to monitor levels of input plasmid DNA. Hirt DNA was isolated as previously described (2), and the samples were digested with *Xho*I or, for the TATA mutants, *Sac*II (New England Biolabs). The samples were run on a 0.8% agarose gel in 1× TBE, transferred to a nylon membrane, and hybridized to the *Xba*I fragment of pIM45, AAV nt 145 to 4518 (49).

The remaining aliquot of cells was used to isolate total RNA as described previously (11). The RNA isolation yields RNA contaminated with plasmid DNA; therefore, the samples were treated with RNase-free DNase I (Worthington Biochemicals) (2).

RNase protection analysis. RNase protections were performed with antisense transcripts from both RP19 and pLK215. RP19 and pLK215 were linearized by digestion with *Sac*II and *Hin*fI, respectively. A 100-ng aliquot of each plasmid was incubated in a 20-μl reaction volume containing 40 mM Tris-HCl (pH 7.9), 6 mM $MgCl_2$, 10 mM dithiothreitol, 2 mM spermidine, 0.5 mM ATP, 0.5 mM GTP, 0.5 mM CTP, 0.025 mM UTP, 50 μCi of [α-^{32}p] UTP (800 Ci/mmol; Amersham), 4 U of RNasin (Promega), and 40 U of T3 RNA polymerase (RP19) or SP6 RNA polymerase (pLK215). The reaction mixtures were incubated at 37°C (T3) or 40°C (SP6) for 1 h. The probes were gel purified on an 6% sequencing gel, eluted (49), and used immediately for hybridization.

Approximately 5 μg of total RNA (A_{260}) was mixed with 2×10^5 cpm of each riboprobe. Hybridization at 55°C and RNase digestion were performed as described previously (43, 48), and the reaction products were analyzed on a 6% sequencing gel. Following electrophoresis, the gels were dried and exposed to film. Bands corresponding to p19 and actin transcripts were quantitated with a Molecular Dynamics ImageQuant version 3.3 PhosphorImager. The final levels of p19 activity were normalized for both actin and input plasmid levels.

Immunoprecipitation experiments. A549 cells grown in 100-mm-diameter dishes were mock transfected or transfected with plasmid pCMVRep78/68. At 36 h posttransfection, nuclear extracts were made (1). An antibody that recognizes only the larger Rep78 and Rep68 proteins (anti-78/68) (22) was coupled to protein A-Sepharose and used as described previously (19). SP1 was detected by immunoblotting with an antibody directed to human SP1 and chemiluminescence (Amersham).

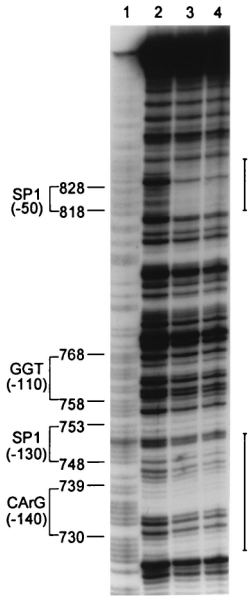

FIG. 2. DNase I footprint of the p19 promoter. A 5′-end-labeled probed containing nt 593 to 906 was used for a Maxam and Gilbert G+A sequencing reaction (lane 1), digestion with DNase I (lane 2), or digestion with DNase I after incubation with 10 μg (lane 3) and 20 μg (lane 4) of a crude HeLa nuclear extract. The products of the reaction were analyzed on a 6% sequencing gel. To the left of the gel, AAV nucleotides are indicated by a single line and putative promoter elements are indicated by brackets and their respective positions in relation to the p19 initiation site. Regions of protection are indicated at the right by horizontal bars.

RESULTS

The SP1 and CArG-like elements are protected from DNase I cleavage. As mentioned above, we previously used deletion mutagenesis to identify four 30-bp regions, nt 720 to 779 and 810 to 869, in the p19 promoter that were necessary for Rep-mediated activation (36). Sequence analysis of this region showed homology to previously characterized transcription factor binding elements (Fig. 1). Two putative TATA boxes were identified at nt 833 to 839 (−35 relative to the start site of transcription) and 843 to 849 (−30), each of which has the potential to direct TATA binding protein interactions and facilitate transcription. Additionally, two putative SP1 binding sites (6) were identified at nt 746 to 753 (−130) and 819 to 831 (−50), and a single CArG-like element (44) was identified at nt 730 to 740 (−140). A GGT box, which has been shown to be a weak SP1 binding element (18, 28, 45), also was identified at nt 758 to 763 (−110). Finally, two putative RBEs were identified (Fig. 1) (36).

Initial characterization of protein interactions at the p19 promoter were performed by DNase I footprinting. Incubation of a 308-bp p19 fragment (nt 598 to 906) with a crude nuclear extract from HeLa cells revealed two distinct regions of protection (Fig. 2). The first region included a portion of the putative SP1 element at −130 and the CArG-like element at −140, both of which were weakly protected. The second was a region of strong protection that included the putative SP1 element at −50. The absence of protection over the TATA elements at positions −30 and −35 was not unexpected. It has

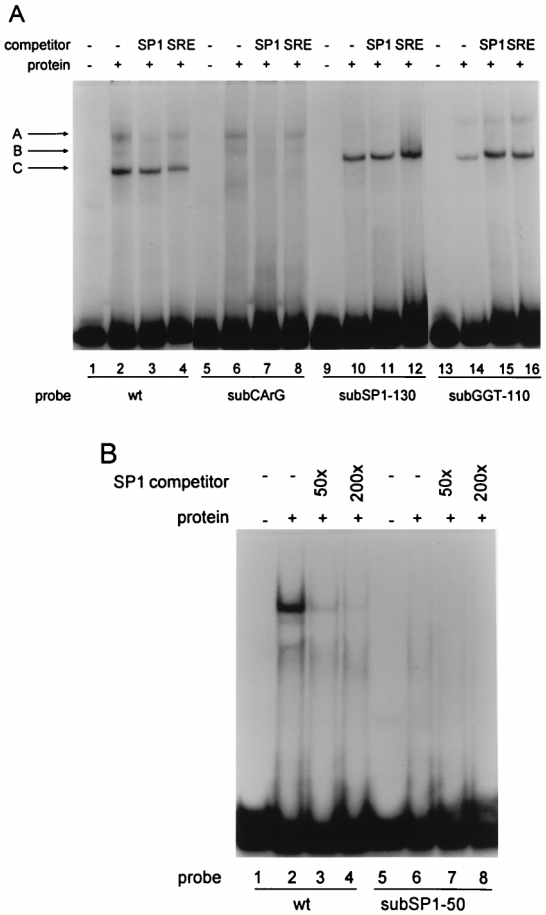

FIG. 3. EMSAs demonstrate interactions with SP1 and a CArG-like element within the p19 promoter. (A) 5′-end-labeled fragment I probes (AAV nt 687 to 814) from the wt p19 promoter (lanes 1 to 4) or p19 clones that had substitutions in the CArG-140 (lanes 5 to 8), SP1-130 (lanes 9 to 12), or GGT-110 (lanes 13 to 16) element were incubated with (lanes 2 to 4, 6 to 8, 10 to 12, and 14 to 16) or without (lanes 1, 5, 9, and 13) a crude HeLa nuclear extract. Reactions in lanes 3, 7, 11, and 15 were challenged with a 200-fold molar excess of an unlabeled SP1 competitor. An unlabeled oligonucleotide containing the c-*fos* SRE was included at a 200-fold molar excess in lanes 4, 8, 12, and 16. The reactions were analyzed on a 4% polyacrylamide gel containing 0.5× TBE. The three retarded complexes, A, B and C, are indicated on the left. (B) A 5′-end-labeled p19 fragment II (AAV nt 815 to 906) from wt (lanes 1 to 4) or a mutant in the SP1-50 site (lanes 5 to 8) was incubated with (lanes 2 to 4 and 6 to 8) or without (lanes 1 and 5) a crude HeLa nuclear extract. Reactions were challenged with 50-fold (lanes 3 and 7) or 200-fold (lanes 4 and 8) molar excess of an unlabeled SP1 competitor where indicated. The products were electrophoresed on a 4% polyacrylamide gel containing 0.5× TBE and 5 mM $MgCl_2$.

been observed that TATA binding protein does not bind efficiently to DNA when in a crude mixture of proteins (42).

Competitive EMSAs experiments demonstrate SP1-p19 interactions. Competitive EMSAs were used to further characterize protein interactions at p19. Incubation of wild-type (wt) p19 fragment II (Fig. 1, AAV nt 815 to 906) resulted in a series of protein-DNA complexes (PDCs) (Fig. 3B, lane 2). These PDCs could be efficiently competed when the reactions were challenged with unlabeled SP1 oligonucleotide (Fig. 3B, lanes 3 and 4). Additionally, the formation of the p19 fragment II PDCs was lost when a probe containing a mutant SP1-50 element was used in place of the wt probe (Fig. 3B, lanes 5 and 6; Table 1). These results were consistent with the strong DNase I protection in this region and suggested that the putative SP1 site at −50 was responsible for the gel shift pattern generated by fragment II.

Incubation of wt p19 fragment I (Fig. 1, AAV nt 687 to 814) with a crude nuclear extract resulted in the formation of three PDCs, A, B, and C (Fig. 3A, lane 2). When the reaction was challenged with an unlabeled SP1 oligonucleotide, the formation of PDCs A and B decreased (Fig. 3A, lanes 3 and 7). In addition, a substitution mutant in the SP1-130 element (Table 1) eliminated both PDC A and PDC B (Fig. 3A, lanes 9 to 12). In contrast, mutation of the GGT-110 element had little effect on the gel shift pattern (Fig. 3A, lanes 13 to 16; Table 1). We concluded that the putative SP1 element at −130 was probably responsible for PDCs A and B.

Fragment I PDC C appeared to be related to the CArG-like element at −140. The formation of PDC C was unaffected by the addition of SP1 competitor or the substitution mutants at −110 and −130 (Fig. 3A). However, a substitution mutant at the CArG-like element at −140 (Table 1) completely eliminated PDC C (Fig. 3A, lanes 6 to 8). Although CArG-like elements are often part of SREs (56), addition of an authentic c-*fos* SRE had little effect on any of the fragment I complexes (Fig. 3A, lanes 4, 8, 12, and 16).

UV cross-linking experiments identify 97-, 105-, and 34-kDa proteins. UV cross-linking experiments were performed to determine the approximate molecular masses of the proteins binding to p19. Two proteins with molecular masses of approximately 97 and 105 kDa were observed in reactions with both fragments I and II (Fig. 4A, lanes 1 and 2). The mobilities of these proteins were consistent with the molecular weights of the phosphorylated and unphosphorylated forms of human SP1 (6). Addition of unlabeled SP1 competitor DNA to the binding reactions reduced the amount of cross-linked SP1 pro-

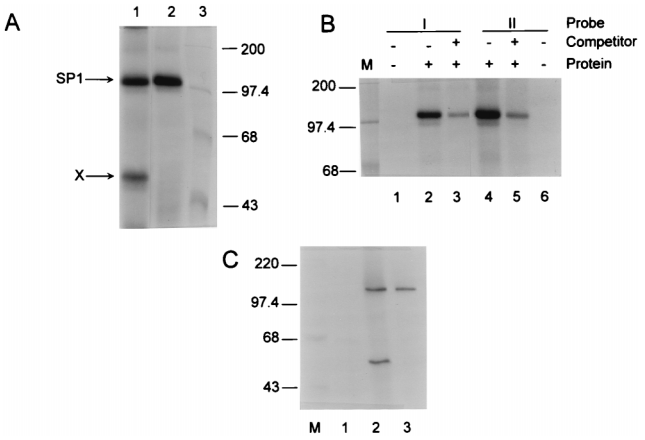

FIG. 4. UV cross-linking experiments of p19 fragments I and II. (A) Uniformly labeled p19 fragments I (lane 1) and II (lane 2) were generated by PCR with [α-^{32}p]dATP incorporated throughout the length of the probe. The substrates were incubated with a crude HeLa nuclear extract and exposed to UV light (λ = 254 nm). Following digestion of unbound DNA, the products were analyzed on an SDS–10% polyacrylamide gel. ^{14}C-labeled molecular weight markers (lane 3) are indicated by their sizes in kilodaltons. Labeled proteins are indicated by arrows as SP1 and X. (B) p19 fragments I (lanes 1 to 3) and II (lanes 4 to 6) were incubated with (lanes 2 to 5) or without (lanes 1 and 6) a crude HeLa nuclear extract. A 300-fold molar excess of an unlabeled SP1 oligonucleotide was included in lanes 3 and 5. The reactions were treated and analyzed as described above. ^{14}C-labeled protein molecular weight markers are indicated in kilodaltons on the left (lane M). (C) p19 fragment I substrates derived from either wt p19 (lanes 1 and 2) or the p19 promoter containing a mutation in the CArG-140 element (lane 3). The uniformly labeled substrates were incubated without (lane 1) or with 30 mg of a crude nuclear extract (lanes 2 and 3), treated, and analyzed as described before. ^{14}C-labeled protein molecular weight markers are indicated in kilodaltons on the left (lane M).

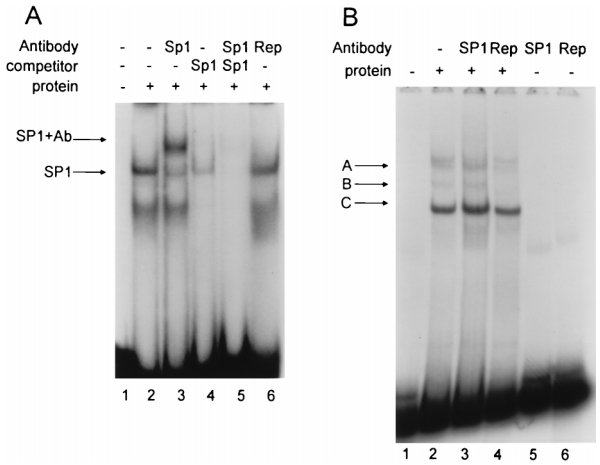

FIG. 5. SP1 antibody addition experiments with p19 fragments I and II. (A) p19 fragment II was incubated without (lane 1) or with (lanes 2 to 6) a crude HeLa nuclear extract (protein). An SP1-specific antibody (lane 3), an unlabeled SP1 oligonucleotide (lane 4), or both antibody and oligonucleotide (lane 5) were added where indicated. A non-SP1 antibody (Rep) was also used (lane 6) as a control. The products were analyzed on a 4% polyacrylamide gel containing 0.5× TBE and 5 mM $MgCl_2$. The positions of SP1 and SP1-antibody (SP1+Ab) PDCs are indicated on the left. (B) p19 fragment I was incubated without (−) or with (+) a crude HeLa nuclear extract where indicated. The SP1 antibody or a control (Rep) antibody was also added to p19 fragment I alone (lanes 5 and 6) or p19 fragment I PDCs (lanes 3 and 4). The reactions were analyzed on a 4% polyacrylamide gel containing 0.5× TBE.

tein from both p19 fragments I and II compared to reactions without competitor (Fig. 4B; compare lanes 2 and 3 and lanes 4 and 5), suggesting that the 97- and 105-kDa proteins were interacting with the SP1 elements in fragments I and II.

In addition to these proteins, a protein with an approximate molecular mass of 48 kDa was observed cross-linked to fragment I (Fig. 4A, lane 1). This interaction was specific for this fragment, as it was not observed with fragment II (Fig. 4A, lane 2). Mutation of the CArG-140 element eliminated cross-linking of the 48-kDa protein to fragment I (Fig. 4C; compare lanes 2 and 3). We concluded that the 48-kDa protein specifically interacted with the CArG-like element. This interaction appeared to be independent of the SP1-130 interaction. Because the 48-kDa cross-linked protein presumably contained approximately 20 bp of DNA, the actual molecular mass of the protein was estimated to be approximately 34 kDa. Indeed, preliminary purification of this protein by affinity chromatography results in the isolation of a 34-kDa protein (not shown).

An SP1 antibody alters the mobility of retarded p19 fragments. To provide further evidence that SP1 was interacting with the p19 promoter fragments, an antibody supershift experiment was performed. As expected, incubation of labeled wt p19 fragment II with a crude extract yielded labeled PDCs (Fig. 5A, lane 2) that were reduced when an unlabeled SP1 competitor was added (Fig. 5A, lane 4). Addition of SP1 antibody to the reaction resulted in the formation of a slower-migrating PDC (Fig. 5A, lane 3) that was not observed if a control antibody was used (Fig. 5A, lane 6). Addition of an unlabeled SP1 competitor to the reaction reduced both the labeled PDC and the antibody containing complex (Fig. 5A, lane 5).

In contrast, incubation of p19 fragment I with a crude extract and SP1 antibody did not produce easily detectable supershifted complexes (Fig. 5B, lanes 2 and 3). There did, however, appear to be a slight qualitative difference in PDCs A and B that was not observed with a control antibody (Fig. 5B; compare lanes 3 and 4), and a small amount of supershifted complex was sometimes seen.

The CArG-140, SP1-130, and SP1-50 elements are necessary for p19 promoter activity. To determine the role of each p19 interaction for promoter activity, we constructed a series of substitution mutations within each of the potential SP1 sites at −130, −110 (GGT), and −50 (Table 1). Additionally, substitution mutants were made within the CArG-like element (−140) and the two TATA sites (−30 and −35) (Fig. 1 and Table 1). All of the mutants were constructed in plasmid pIM45, which contains the wt AAV sequence but is missing the TRs. With the exception of the two TATA mutants, each mutant also contained a stop codon at the substitution site so that it was incapable of making functional Rep78 or Rep68 (Table 1). To assess the effect of each mutant on p19 transcription, the mutants were cotransfected with a plasmid, p19/40S, that supplied wt Rep in *trans* (36). p19/40S contained a series of third-position codon changes that did not alter the amino acid composition of the Rep proteins but did allow for discrimination between the p19 transcripts synthesized from the promoter mutants and p19/40S (Fig. 6). Riboprobe hybridized to the promoter mutant transcripts produced a protected fragment of 175 bp, while p19/40S transcripts produced two fragments of 86 and 69 bp (Fig. 6 and Fig. 7A and B). A riboprobe to γ-actin was used to normalize total RNA recovery (Fig. 7A),

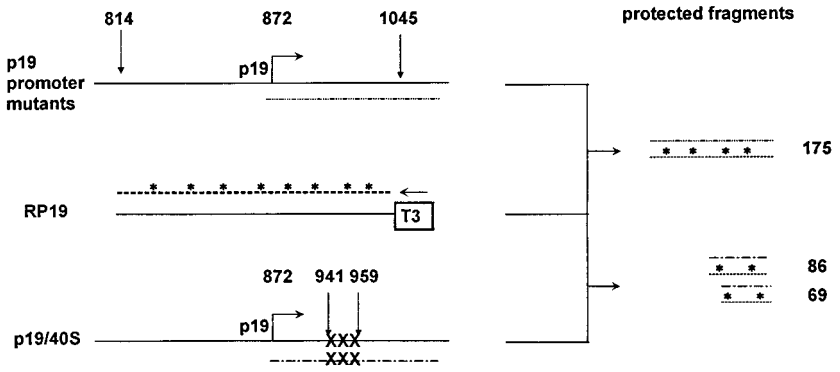

FIG. 6. Schematic of the p19 RNase protection assay. p19 transcripts from the p19 promoter mutants initiate at nt 872 and, when hybridized to the T3-transcribed RP19 antisense RNA (AAV nt 1045 to 814), yield a 175-bp RNase-resistant fragment. Transcripts from the p19/40S template also initiate at nt 872; however, mutations between nt 941 and 959 prevent complete hybridization to the RP19 antisense RNA, and subsequent RNase digestion of these hybrids results in 86- and 69-bp protected fragments. See Materials and Methods for further details.

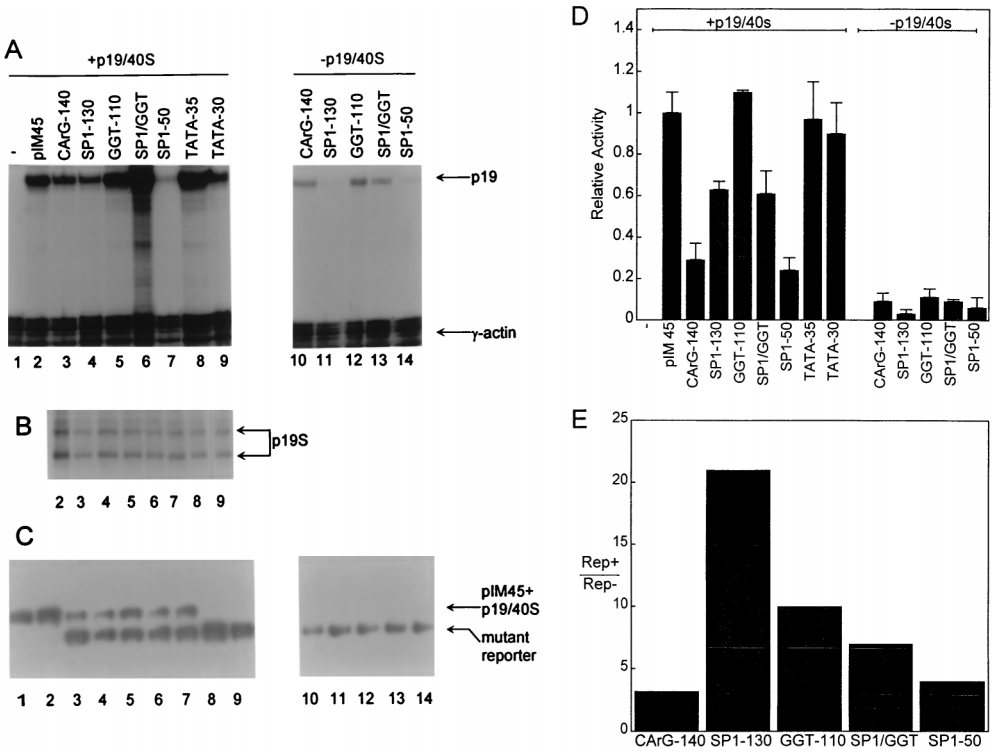

FIG. 7. RNase protection analysis of p19 promoter mutations in the presence or absence of wt Rep. (A) A549 cells were transfected with 5 μg of the *rep*$^+$ plasmid, p19/40S (lanes 1–9), no reporter (−; lane 1), 5 μg of the wild-type pIM45 reporter plasmid (lane 2), or 5 μg of a plasmid containing a mutation in one of the p19 promoter elements (CArG-140, SP1-130, GGT-110, both SP1-130 and GGT-110 [SP1/GGT], SP1-50, TATA-35, or TATA-30; lanes 3 to 9). The cells also were infected with Ad at a multiplicity of infection of 5. Some of the p19 promoter mutants (5 μg) were also transfected in the absence of the *rep*$^+$ plasmid p19/40S (lanes 10 to 14) and infected with Ad. Forty hours posttransfection, RNA was isolated and measured by RNase protection. The positions of the 175-bp p19 and the 135-bp γ-actin protected fragments are indicated by arrows. (B) Analysis of p19 transcription from the p19/40S template. RNA from the experiment panel A (lanes 2 to 9) was analyzed by RNase protection using the RP19 riboprobe; the 69- and 86-bp protected fragments are indicated on the right. (C) Ten percent of the transfected cells from the experiment in panel A (lanes 1 to 14) were used to isolate and quantitate input plasmid DNA. Hirt DNA was digested with *Sac*II (TATA mutants) or *Xho*I (other mutants), run on a 0.7% agarose gel, and blotted onto a nylon membrane. The blots were hybridized to a radiolabeled DNA fragment containing AAV nt 190 to 4487. Indicated on the right are the positions of the pIM45 and p19/40S plasmids and the p19 mutant plasmids. Digestion of the p19/40S plasmid with *Sac*II yields a fragment with a mobility similar to that of the *Sac*II fragment of the TATA mutants, and therefore these fragments are not separated on this gel. The levels of the p19 TATA mutant reporter plasmids were estimated from the plasmid levels in the other p19 mutant transfections by subtracting the average amount of p19/40S plasmid from the total plasmid DNA. (D) Three independent experiments monitoring p19 promoter activity were normalized for levels of both total RNA (γ-actin) and input plasmid DNA. The average level of p19 transcript from the wt p19 promoter in pIM45 in the presence of p19/40S (+p19/40S) was arbitrarily set to 1. Then, the average levels of p19 transcripts from the p19 promoter mutants in the presence (+) or absence (−) of p19/40S were calculated relative to the level for pIM45. The error bars indicate the maximum deviation from the mean. (E) The ratios of p19 promoter activity from the p19 mutants CArG-140, SP1-130, GGT-110, and SP1-50 and the double mutant SP1/GGT in the presence of p19/40S (Rep+) versus the absence of p19/40S (Rep−) were calculated and plotted.

and Hirt extraction of input plasmid DNA was used to normalize transfection efficiency (Fig. 7C). The average of three experiments was then normalized to the value for wt parental plasmid, pIM45 (Fig. 7D).

Three of the mutants, CArG-140, SP1-130, and SP1-50, were found to have a significant effect on p19 transcription, approximately two- to threefold each. This result was consistent with the DNase I protection assays and EMSAs described above, which demonstrated that these sites were bound by SP1 or a 48-kDa protein and suggested that these three positions were necessary for p19 promoter activity. Disruption of either of the two TATA elements had no significant effect on p19 activity, suggesting that these two elements were redundant. Additionally, mutation of the GGT element at −110 also appeared to have no effect on p19 promoter activity, either by itself or in combination with a mutation in the nearby SP1-130 element (Fig. 7D).

Conceivably, one or more of the SP1 sites or the CArG-like element were responsible for mediating activation of the p19 promoter by Rep78/68. To see if this was the case, the level of p19 activity in the absence of the complementing p19/40S plasmid was measured (Fig. 7A) and the ratio of p19 activity in the presence and absence of Rep78/68 was calculated (Fig. 7E). We reasoned that if a particular sequence element was involved in Rep-mediated activation of p19, then mutation of that element would reduce the effect of Rep on p19 promoter activity. Thus, a ratio closer to 1 would indicate that the mutated element was more likely to be involved in Rep-mediated p19 transactivation, and a ratio of exactly 1 would indicate that the mutated element was the only sequence responsible for the Rep response.

All of the mutants displayed more p19 activity in the presence of Rep78/68 than they did in absence of the p19/40S plasmid, suggesting that no one element was uniquely responsible for Rep activation. The CArG-140 mutant and SP1-50 mutant showed relatively modest increases in the presence of Rep, three- and fourfold, respectively. This finding suggested that the contribution of these elements to p19 promoter activity was more dependent on the presence of Rep. In contrast, the SP1-130 and GGT-110 sites appeared to have a more normal response to Rep (i.e., both were activated 10- to 20-fold), suggesting that mutation of these two elements did not

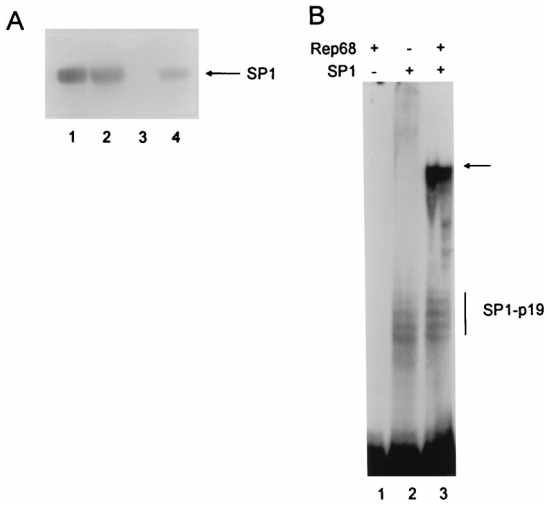

FIG. 8. Direct interaction between Rep78/68 and the cellular factor SP1. (A) One-fifth of a nuclear extract from A549 cells that were mock transfected (lane 1) or transfected with 5 μg of pCMVRep78/68 (lane 2) was electrophoresed on an SDS–10% polyacrylamide gel. In addition, a Sepharose-coupled antibody that recognizes only Rep78/68 (23) was added to the remainder of the mock-transfected (lane 3) or pCMVRep78/68-transfected (lane 4) extracts. Proteins bound to the antibody-Sepharose beads were boiled in 2× SDS loading buffer and electrophoresed on the same SDS-gel. Following electrophoresis, immunoblotting was performed with an antibody specific for human SP1. The position of SP1 is indicated by an arrow. (B) p19 fragment II was incubated with purified Rep68 (lane 1, 23 ng of Rep), purified SP1 (lane 2, 0.7 footprinting units [Promega]), or both SP1 and Rep68 (lane 3). The reaction mixtures were electrophoresed on a 5% acrylamide gel containing 0.5× TBE. SP1-p19 PDCs are indicated by a vertical line, and a Rep-SP1-dependent PDC is indicated by an arrow.

significantly affect Rep transactivation. We note, however, that this kind of analysis does not provide information about the relative contribution of each element to p19 promoter activity in the absence of Rep78/68. Thus, it is possible that the SP1-130 element contributes the most to basal p19 transcription.

Each of the mutants discussed above synthesized a truncated Rep protein which might have a dominant negative effect on p19 transactivation and could confuse the interpretation of the results. To rule out this possibility, we examined the effects of all the mutants and the wt pIM45 plasmid on transcription from the p19/40S plasmid. No effect was seen in *trans* on p19 transcription from the p19/40S plasmid (Fig. 7B).

SP1 directly interacts with Rep 78/68 and facilitates Rep interaction with the p19 promoter. It seemed likely that the SP1 interaction at position −50 was necessary for mediating Rep activation of p19; however, it was not apparent how SP1 mediates Rep induction of the p19 promoter. It was possible that Rep interacts with p19-bound SP1 and stimulates p19 activity without direct DNA contact. Alternatively, SP1 could stabilize a direct interaction between Rep and p19 DNA. In either case, Rep would have to be capable of making direct contacts with SP1. To determine if SP1 and Rep78/68 could interact with each other, an immunoprecipitation experiment was performed with a monoclonal antibody that recognizes Rep78/68. Nuclear extracts were made from cells that were mock transfected or transfected with pCMVRep78/68. Both extracts contained approximately the same levels of cellular SP1 (Fig. 8A, lanes 1 and 2). When these extracts were incubated with the anti-78/68 antibody, the precipitate from the extract that contained Rep78/68 also contained SP1 (Fig. 8A, lane 4). This was not true of the mock-transfected extract, which suggested that Rep78 or Rep68 could form a protein complex with at least a portion of the intracellular SP1 in vivo.

To determine whether this interaction could occur when SP1 was bound to a p19 promoter fragment, we examined whether Rep could supershift a p19-SP1 PDC. We established earlier in this report that SP1 binds well to p19 fragment II, and as expected, incubation of this probe with purified SP1 resulted in the formation of several PDCs (Fig. 8B, lane 2). Purified Rep68 alone had no detectable binding activity in this experiment (Fig. 8B, lane 1), consistent with its low affinity for p19 (38) (see below). However, if Rep was added to a binding reaction containing SP1, a new distinct set of PDCs was observed (Fig. 8B, lane 3). This result suggested that Rep could interact with SP1 when it is bound to the SP1 site at −50.

Relative affinity of Rep68 to p5, p19, p40, and the TR. We previously demonstrated that purified Rep68 interacts with a linear 22-bp sequence within the TR and the p5 promoter (38). Additionally, there appeared to be weaker interactions with the p19 and p40 promoter regions, and RBE-like sequences were found in both of these promoters (Fig. 1). To determine the relative affinity of Rep68 to the TR and the p5, p19, and p40 promoters, we did competition EMSAs as described previously (39). Unlabeled oligonucleotides containing the p5, p19, p40, and TR RBEs were used to compete the binding of Rep68 to a linear TR RBE substrate. The K_d of the p5 promoter was found to be approximately 20-fold higher than that of the linear RBE within the TR (Fig. 9). The relative K_ds of the p19 and p40 promoters were determined by comparison to p5 due to the weakness of the p19 and p40 interactions and were then extrapolated to the TR RBE. Rep68 was found to have approximately 160- and 80-fold-lower affinity for the p19 and p40 promoters, respectively, than the linear TR RBE substrate.

DISCUSSION

To understand the mechanism by which AAV Rep proteins regulate transcription from the p19 promoter, we characterized the cellular factors and proximal sequence elements that

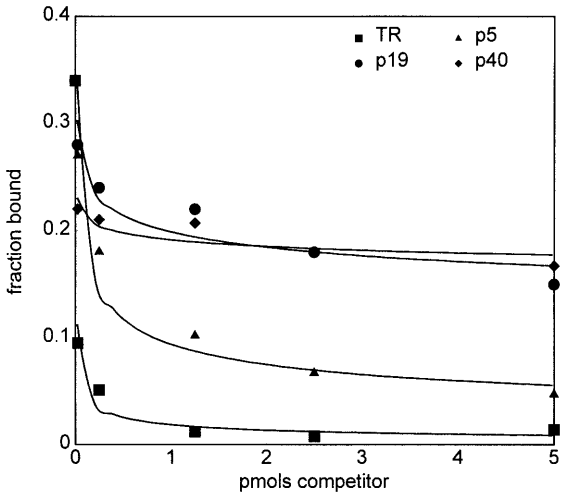

FIG. 9. The relative K_ds of p5, p19, and p40 substrates compared to the TR RBE (A-stem) substrate. An oligonucleotide containing the TR RBE was 5′-end labeled, and 0.025 pmol was used as the binding substrate for 60 ng of Rep68. Unlabeled TR, p5, p19, and p40 substrates were used as competitors for binding to the labeled TR RBE substrate and added at 0.025, 0.25, 1.25, 2.5 and 5 pmol per reaction. Following electrophoresis and autoradiography, bands corresponding to bound and free labeled substrate were cut from the gel and counts per minute was measured in a scintillation counter. The fraction bound was calculated and plotted as a function of picomoles of competitor.

are required for p19 promoter activity. In a previous study, we used deletion analysis to identify four 30-bp regions (Fig. 1) that were necessary for p19 activity in the presence of Rep protein (38). Several putative transcription factor binding elements, including two TATA boxes, two SP1 sites, a GGT box, and a CArG-like element, were identified in these regions. In this study, we used substitution mutants and a variety of biochemical techniques to assess the role of these putative transcription elements in controlling p19 transcription. We concluded that (in addition to one or both of the TATA sites) at least three of these elements, the SP1 site at −50 relative to the start of transcription, a second SP1 site at −130, and the CArG-like element at −140, were important for p19 activity. Additionally, we show that the p19 promoter was capable of a weak interaction with purified Rep68. This interaction may be directed by two potential RBEs (Fig. 1) that were identified by sequence homology (38).

SP1-50 site. DNase I footprinting analysis demonstrated that the putative SP1 element at −50 relative to the start of transcription was protected from DNase I cleavage. EMSAs using mutant substrates, specific oligonucleotide competitors, and SP1 antibodies, in addition to UV cross-linking experiments, clearly demonstrated that SP1 interacts with the SP1-50 element in the p19 promoter.

The SP1-50 interaction was necessary for p19 activity in both the absence and the presence of Rep78/68 and was one of two sites (the other being the CArG element) that was particularly sensitive to Rep induction of p19 transcription. Because the SP1-50 site overlaps a putative RBE, it was difficult to completely exclude the possibility that the phenotype of the SP1-50 mutant was due to altered Rep binding rather than altered SP1 binding. However, several lines of evidence suggested that SP1 binding at the −50 site is essential for both basal p19 promoter activity and Rep transactivation of p19. First, Rep bound to p19 DNA with approximately 160-fold-lower affinity than to the TR RBE, and relatively high concentrations of purified Rep were required to detect a stable Rep-p19 complex (38) (Fig. 8). Second, we have been unable to demonstrate that purified Rep protects either the region containing the SP1-50 site or the region containing the site of transcript initiation from DNase digestion (not shown). In contrast, both purified and crude forms of SP1 bound readily to the SP1-50 site. Third, analysis of mutants in the two TATA boxes within the p19 promoter, including the one which overlaps the putative RBE, suggested that both TATA boxes were functional (see below). Finally, SP1 and Rep could form a stable complex in vivo as demonstrated by immunoprecipitation. Furthermore, SP1 binding to the −50 site facilitated Rep interaction with the p19 promoter, presumably through protein-protein contacts. These results suggested that Rep by itself does not bind to the p19 promoter under physiological conditions and that the complex formed between Rep, SP1, and p19 DNA is required for Rep transactivation of the p19 promoter.

SP1-130. SP1 (or an SP1-like protein) also appeared to bind to the element at −130, although not as strongly as the −50 site. Both DNase I protection and gel shift experiments suggested that this site was bound more weakly than the site at −50. Cross-linking experiments (Fig. 4) demonstrated an interaction between the −130 site and a protein similar in size to human SP1 (6), and oligonucleotide competition experiments and gel shift experiments using a substrate with a mutant −130 site (Fig. 3 and 4) also supported an interaction between SP1 and the −130 site. However, antibody supershift experiments did not conclusively confirm the presence of SP1. This may have been due to the presence of other proteins bound near or at the −130 site which interfered with antibody recognition, or it may have been due to the presence of a different protein bound to the −130 site. Two reports have identified SP1-related genes with binding characteristics similar to those of SP1. One gene, SPR2 (28) or SP3 (18), encodes a protein with a predicted molecular mass of approximately 100 kDa (SP1 is approximately 97 kDa) and is expressed in a variety of cell types, including HeLa cells. Thus, it is possible that this SPR3/SP2 protein is responsible for the interactions that we observed with the p19 SP1-130 element.

While the identity of the protein that interacts with the SP1-130 element was not conclusively demonstrated, the element and its associated transcription factor appeared to be required for maximal p19 activity. Unlike the SP1-50 site, the −130 element appeared to be relatively independent of Rep activity, and we concluded that it was more likely to contribute to p19 promoter activity by increasing the basal rate of transcription.

CArG-140. The third element which appeared to have a strong effect on p19 promoter activity was a CArG-like site at position −140. This element was found to interact with a protein that was present in crude HeLa cell extracts and had an approximate molecular mass of 34 kDa. Although the CArG-like element was near the SP1-130 site, EMSA and UV cross-linking experiments suggested that the protein that interacts with this site is independent of the SP1 promoter element. The CArG element was not part of an SRE site, as competition experiments with an authentic SRE site were not successful. Because we are unaware of a 34-kDa transcription factor that can bind to a CArG-like sequence, we tentatively concluded that this protein is a novel transcription factor and have called it cAAP. Analysis of transcription factor binding sites (5), in particular CArG elements, has not provided any additional information about the identity of cAAP. In addition to the oligonucleotide experiments using SP1 and SRE, several competitive EMSAs using oligonucleotides corresponding to a variety of other transcription factor elements, including YY1 (50), major late transcription factor (9), ATF (14), EF1A (7), and RBE (38), were unable to disrupt the cAAP interaction (data not shown). Furthermore, we have determined that the CArG-140 element alone (i.e., the sequence CCAGAAATGG shown in Fig. 1) cannot compete for cAAP binding to p19 promoter DNA; 5 to 6 additional bp 5′ of the CArG element are required for this interaction (data not shown).

A substitution mutant within the CArG site demonstrated that it contributes to p19 promoter activity and, like the SP1-50 element, mediates Rep activation of the p19 promoter. Although we have not yet determined whether Rep and cAAP interact, we would speculate that cAAP facilitates Rep transactivation through protein interactions, like the SP1-50 interactions.

Redundant TATA sites. Mutation of either of the two TATA sites in the p19 promoter (−30 or −35) had no effect on p19 promoter activity. This result confirmed the previous results of Chejanovsky and Carter (10), who also demonstrated that either TATA site could be mutated without affecting p19 activity, and suggested that the two TATA sites are redundant. In contrast, we previously reported that deletion of nt 840 to 869 (*dl*810 [Fig. 1]), which included the TATA site at −30, completely abolished p19 promoter activity (36). The apparent discrepancy may be due to the fact that the deletion positioned the remaining −35 TATA site only 8 bp from the start of transcription initiation. Alternatively, it may reflect the need for the putative RBE at the site of transcription initiation (Fig. 1). The latter seems unlikely because it is difficult to see how Rep binding at the transcription initiation site would do anything but inhibit p19 activity. Nevertheless, we have not yet

tested mutants in the putative Rep binding site at nt 864 to 888 to rule out this possibility.

With the exception of *dl*840, our results in this study are consistent with the deletion analysis of the p19 promoter that we reported previously (36). The cAAP binding site and the SP1-130 site (Fig. 1) would account for the phenotypes of *dl*720 (deletion of nt 720 to 749) and *dl*750 (nt 750 to 779). Similarly, the SP1-50 site would account for the phenotype of *dl*810 (nt 810 to 839).

Mechanism of Rep transactivation of p19. In addition to the proximal p19 promoter elements that we identified in this study, we previously observed that Rep78/68 interactions with either the p5 RBE or the TR RBE are required for both p19 and p40 transactivation (43). We proposed that Rep78/68 that is bound to these RBEs interacts directly with p19-bound cellular transcription factors to achieve Rep transactivation of p19. The formation of these complexes would result in the looping out of the intervening DNA, similar to those described for other transcriptional enhancer elements (35). The evidence presented here that Rep can make direct protein contacts with SP1 support the idea of a p5-Rep-SP1-p19 complex that could account for Rep transactivation of the p19 promoter.

ACKNOWLEDGMENTS

We thank Xiaohuai Zhou for constructing the pCMVRep78/68 construct.

This work was supported by grants PO1 CA2814607, RO1 GM3572302, and HL/DK 50257 from the National Institutes of Health to N.M., by support from the American Cancer Society E. M. Koger Fund to N.M., and by Public Health Service training grant T32 AI25530 to D.J.P.

REFERENCES

1. **Andrews, N. C., and D. V. Faller.** 1991. A rapid micropreparation technique for extraction of DNA-binding proteins from limiting numbers of mammalian cells. Nucleic Acids Res. **19:**2499.
2. **Ausubel, F. M., R. Brent, R. E. Kingston, D. D. Moore, J. G. Seidman, J. A. Smith, and K. Struhl (ed.).** 1995. Current protocols in molecular biology. Greene Publishing Associates, Brooklyn, N.Y.
3. **Becerra, S. P., F. Koczot, P. Fabisch, and J. A. Rose.** 1988. Synthesis of adeno-associated virus structural proteins requires both alternative mRNA splicing and alternative initiations from a single transcript. J. Virol. **62:** 2745–2754.
4. **Becerra, S. P., J. A. Rose, M. Hardy, B. M. Baroudy, and C. W. Anderson.** 1985. Direct mapping of adeno-associated virus capsid proteins B and C: a possible ACG initiation codon. Proc. Natl. Acad. Sci. USA **82:**7919–7923.
5. **Boulikas, T.** 1994. A compilation and classification of DNA binding sites for protein transcription factors from vertebrates. Crit. Rev. Eukaryotic Gene Expression **2:**117–321.
6. **Briggs, M. R., J. T. Kadonaga, S. P. Bell, and R. Tjian.** 1986. Purification and biochemical characterization of the promoter-specific transcription factor SP1. Science **234:**234–4772.
7. **Bruder, J. T., and P. Hearing.** 1989. Nuclear factor EF-1A binds to the adenovirus E1aA core enhancer element and to other transcriptional control regions. Mol. Cell. Biol. **9:**5143–5153.
8. **Casto, B. C., R. W. Atchison, and W. M. Hammon.** 1967. Studies on the relationship between adeno-associated virus type I (AAV-1) and adenoviruses. I. Replication of AAV-1 in certain cell cultures and its effect on helper adenovirus. Virology **32:**52–59.
9. **Chang, L. S., Y. Shi, and T. Shenk.** 1989. Adeno-associated virus P5 promoter contains an adenovirus E1A-inducible element and a binding site for the major late transcription factor. J. Virol. **63:**3479–3488.
10. **Chejanovsky, N., and B. J. Carter.** 1989. Mutagenesis of an AUG codon in the adeno-associated virus rep gene: effects on viral DNA replication. Virology **173:**120–128.
11. **Chomezynski, P., and N. Sacchi.** 1987. Single-step method of RNA isolation by acid guanidinium thiocyanate-phenol-chloroform extraction. Anal. Biochem. **162:**156–159.
12. **Clark, K. R., F. Voulgaropoulou, D. M. Fraley, and P. R. Johnson.** 1995. Cell lines for the production of recombinant adeno-associated virus. Hum. Gene Ther. **6:**1329–1341.
13. **Dignan, J. D., R. M. Lebovitz, and R. G. Roeder.** 1983. Accurate transcription initiation by RNA polymerase II in a soluble extract from isolated mammalian nuclei. Nucleic Acids Res. **11:**1475–1486.
14. **Flint, J., and T. Shenk.** 1989. Adenovirus E1A protein: paradigm viral transactivator. Annu. Rev. Genet. **23:**141–161.
15. **Gao, X., and L. Huang.** 1991. A novel cationic liposome reagent for efficient transfection of mammalian cells. Biochem. Biophys. Res. Commun. **179:** 280–285.
16. **Green, M. R., and R. G. Roeder.** 1980. Transcripts of the adeno-associated virus genome: mapping of the major RNAs. J. Virol. **36:**79–92.
17. **Green, M. R., and R. G. Roeder.** 1980. Definition of a novel promoter for the major adeno-associated virus mRNA. Cell **1:**231–242.
18. **Hagen, G., S. Muller, M. Beato, and G. Suske.** 1992. Cloning by recognition site screening of two novel GT box binding proteins: a family of SP1 related genes. Nucleic Acids Res. **20:**5519–5525.
19. **Harlow, D., and E. Lane.** 1988. Antibodies. A laboratory manual. Cold Spring Harbor Laboratory Press, Cold Spring Harbor, N.Y.
20. **Hermonat, P. L., M. A. Labow, R. Wright, K. I. Berns, and N. Muzyczka.** 1984. Genetics of adeno-associated virus: isolation and preliminary characterization of adeno-associated virus type 2 mutants. J. Virol. **51:**329–339.
21. **Horer, M., S. Weger, K. Butz, F. Hoppe-Seyler, C. Geisen, and J. A. Kleinschmidt.** 1995. Mutational analysis of adeno-associated virus Rep protein-mediated inhibition of heterologous and homologous promoters. J. Virol. **69:**5485–5496.
22. **Hunter, L. A., and R. J. Samulski.** 1992. Colocalization of adeno-associated virus Rep and capsid proteins in nuclei of infected cells. J. Virol. **66:**317–324.
23. **Hunter, L. A., and R. J. Samulski.** 1992. Colocalization of adeno-associated virus Rep and capsid proteins in the nuclei of infected cells. J. Virol. **66:**317–324.
24. **Im, D. S., and N. Muzyczka.** 1990. The AAV origin binding protein Rep68 is an ATP-dependent site-specific endonuclease with DNA helicase activity. Cell **61:**447–457.
25. **Im, D. S., and N. Muzyczka.** 1992. Partial purification of adeno-associated virus Rep78, Rep52, and Rep40 and their biochemical characterization. J. Virol. **66:**1119–1128.
26. **Janik, J. E., M. M. Huston, and J. A. Rose.** 1984. Adeno-associated virus proteins: origin of the capsid components. J. Virol. **52:**591–597.
27. **Johnson, P. F., and S. L. McKnight.** 1989. Eukaryotic transcritpional regulatory proteins. Annu. Rev. Biochem. **58:**799–839.
28. **Kingsley, C., and A. Winoto.** 1992. Cloning of GT box-binding proteins: a novel SP1 multigene family regulating T-cell receptor gene expression. Mol. Cell. Biol. **12:**4251–4261.
29. **Kunkel, T. A.** 1985. Rapid and efficient site-specific mutagenesis without phenotypic selection. Proc. Natl. Acad. Sci. USA **82:**488–492.
30. **Kyostio, S. R. M., R. A. Owens, M. D. Weitzman, B. A. Antoni, N. Chejanovsky, and B. J. Carter.** 1994. Analysis of adeno-associated virus (AAV) wild-type and mutant Rep proteins for their abilities to negatively regulate AAV p5 and p19 mRNA levels. J. Virol. **68:**2947–2957.
31. **Kyostio, S. R. M., R. S. Wonderling, and R. A. Owens.** 1995. Negative regulation of the adeno-associated virus (AAV) P5 promoter involves both the p5 Rep binding site and the consensus ATP-binding motif of the AAV Rep68 protein. J. Virol. **69:**6787–6796.
32. **Labow, M. A., P. L. Hermonat, and K. I. Berns.** 1986. Positive and negative autoregulation of the adeno-associated virus type 2 genome. J. Virol. **60:** 251–258.
33. **Laughlin, C. A., N. Jones, and B. J. Carter.** 1982. Effect of deletions in adenovirus region 1 genes upon replication of adeno-associated virus. J. Virol. **41:**868–876.
34. **Lewis, B. A., G. Tullis, E. Seto, N. Horikoshi, R. Weinmann, and T. Shenk.** 1995. Adenovirus E1A proteins interact with the cellular YY1 transcription factor. J. Virol. **69:**1628–1636.
35. **Matthews, K. S.** 1992. DNA looping. Microbiol. Rev. **56:**123–136.
36. **McCarty, D. M., M. Christensen, and N. Muzyczka.** 1991. Sequences required for coordinate induction of adeno-associated virus p19 and p40 promoters by Rep protein. J. Virol. **65:**2936–2945.
37. **McCarty, D. M., T. H. Ni, and N. Muzyczka.** 1992. Analysis of mutations in adeno-associated virus Rep protein in vivo and in vitro. J. Virol. **66:**4050–4057.
38. **McCarty, D. M., D. J. Pereira, I. Zolotukhin, X. Zhou, J. H. Ryan, and N. Muzyczka.** 1994. Identification of linear DNA sequences that specifically bind the adeno-associated virus Rep protein. J. Virol. **68:**4988–4997.
39. **McCarty, D. M., J. H. Ryan, S. Zolotukhin, X. Zhou, and N. Muzyczka.** 1994. Interaction of the adeno-associated virus Rep protein with a sequence within the A palindrome of the viral terminal repeat. J. Virol. **68:**4998–5006.
40. **McPherson, R. A., L. J. Rosenthal, and J. A. Rose.** 1985. Human cytomegalovirus completely helps adeno-associated virus replication. Virology **147:** 217–222.
41. **Mendelson, E., J. P. Trempe, and B. J. Carter.** 1986. Identification of the *trans*-acting Rep proteins of adeno-associated virus by antibodies to a synthetic oligopeptide. J. Virol. **60:**823–832.
42. **Nakajima, N., M. Horikoshi, and R. G. Roeder.** 1988. Factors involved in specific transcription by mammalian RNA polymerase II: purification, genetic specificity, and TATA box-promoter interactions of TFIID. Mol. Cell. Biol. **8:**4028–4040.

43. **Pereira, D. J., D. M. McCarty, and N. Muzyczka.** 1997. The adeno-associated virus (AAV) Rep protein acts as both a repressor and an activator to regulate AAV transcription during a productive infection. J. Virol. **71:** 1079–1088.
44. **Phan-Din-Tuy, F., F. Tuil, and A. Minty.** 1988. The CC.Ar.GG box, a protein binding site common to transcriptional-regulatory regions of the cardiac actin, c-fos and interleukin-2 receptor genes. Eur. J. Biochem. **173:**507–515.
45. **Pitluk, Z. W., and D. C. Ward.** 1991. Unusual Sp1-GC box interaction in a parvovirus promoter. J. Virol. **65:**6661–6670.
46. **Richardson, W. D., and H. Westphal.** 1984. Requirement for either early region 1a or early region 1b adenovirus gene products in the helper effect for adeno-associated virus. J. Virol. **51:**404–410.
47. **Richardson, W. D., and H. Westphal.** 1984. Adenovirus early gene regulation and the adeno-associated virus helper effect. Curr. Top. Microbiol. Immunol. **109:**147–165.
48. **Saccomanno, C. F., M. Bordonaro, J. S. Chen, and J. L. Nordstrom.** 1992. A faster ribonuclease protection assay. BioTechniques **13:**846–850.
49. **Sambrook, J., E. F. Fritsch, and T. Maniatis.** 1989. Molecular cloning: a laboratory manual, 2nd ed. Cold Spring Harbor Laboratory Press, Cold Spring Harbor, N.Y.
50. **Shi, Y., E. Seto, L. S. Chang, and T. Shenk.** 1991. Transcriptional repression by YY1, a human GLI-Kruppel-related protein, and relief of repression by adenovirus E1A protein. Cell **67:**377–388.
51. **Snyder, R. O., R. J. Samulski, and N. Muzyczka.** 1990. In vitro resolution of covalently joined AAV chromosome ends. Cell **60:**105–113.
52. **Srivastava, A., E. W. Lusby, and K. I. Berns.** 1983. Nucleotide sequence organization of the adeno-associated virus 2 genome. J. Virol. **45:**555–564.
53. **Tratschin, J. D., I. L. Miller, and B. J. Carter.** 1984. Genetic analysis of adeno-associated virus: properties of deletion mutants constructed in vitro and evidence for an adeno-associated virus replication function. J. Virol. **51:**611–619.
54. **Tratschin, J. D., M. H. West, T. Sandbank, and B. J. Carter.** 1984. A human parvovirus, adeno-associated virus, as a eucaryotic vector: transient expression and encapsidation of the procaryotic gene for chloramphenicol acetyltransferase. Mol. Cell. Biol. **4:**2072–2081.
55. **Trempe, J. P., E. Mendelson, and B. J. Carter.** 1987. Characterization of adeno-associated virus rep proteins in human cells by antibodies raised against rep expressed in Escherichia coli. Virology **61:**18–28.
56. **Triesman, R.** 1990. The SRE: a growth factor response transcriptional regulator. Semin. Cancer Biol. **1:**47–58.
57. **West, M. H. P., J. P. Trempe, J.-D. Tratschin, and B. J. Carter.** 1987. Gene expression in adeno-associated virus vectors: the effects of chimeric mRNA structure, helper virus, and adenovirus VAI RNA. Virology **160:**38–47.
58. **Wonderling, R. S., S. R. Kyostio, and R. A. Owens.** 1995. A maltose-binding protein/adeno-associated virus Rep68 fusion protein has DNA-RNA helicase and ATPase activities. J. Virol. **69:**3542–3548.
59. **Yang, Q., A. Kadam, and J. P. Trempe.** 1992. Mutational analysis of the adeno-associated virus *rep* gene. J. Virol. **66:**6058–6069.